J|A|C|S ARTICLES

Published on Web 12/10/2008

Creating Conformational Entropy by Increasing Interdomain Mobility in Ligand Binding Regulation: A Revisit to N-Terminal Tandem PDZ Domains of PSD-95

Wenning Wang,*,†,‡ Jingwei Weng,† Xu Zhang,§ Maili Liu,§ and Mingjie Zhang*,‡,||

Department of Chemistry and Institute of Biomedical Sciences, Fudan University, Shanghai, 200433, China, State Key Laboratory of Magnetic Resonance and Atomic and Molecular Physics, Wuhan Institute, of Physics and Mathematics, Chinese Academy of Sciences, Wuhan 430071 China, and Department of Biochemistry, Hong Kong University of Science and Technology, Clear Water Bay, Kowloon, Hong Kong

Received September 24, 2008; E-mail: wnwang@fudan.edu.cn; mzhang@ust.hk

Abstract: The two N-terminal PDZ domains of postsynaptic density protein-95 (PDS-95 PDZ1 and PDZ2) are closely connected in tandem by a conserved peptide linker of five amino acids. The interdomain orientation between PDZ1 and PDZ2 of the ligand-free PDZ12 tandem is restrained, and this conformational arrangement facilitates the synergistic binding of PDZ12 to multimeric targets.[1] The interdomain orientation of the target-bound state of PDZ12 is not known. Here, we have solved the structure of PDZ12 in complex with its binding domain from cypin. Both chemical shift data and residual dipolar coupling measurements showed that the restrained interdomain orientation disappeared upon cypin peptide binding. NMR-based relaxation experiments revealed slow interdomain motions in the PDZ12/cypin peptide complex. Molecular dynamics simulations also showed that the PDZ12/cypin complex has larger conformational flexibility than the ligand-free PDZ12. This dramatic change of protein dynamics provides extra conformational entropy upon ligand binding, thus enhancing the ligand binding affinity of the PDZ12 tandem. Modulation of ligand binding affinity through concerted interdomain structural and dynamic rearrangements may represent a general property of multidomain scaffold proteins.

Introduction

PDZ domain is one of the most common protein−protein interaction modules in the genomes of eukaryotes. PDZ domain-containing proteins play important roles in organizing signal transduction complexes, clustering membrane receptors, and maintaining cell polarities.[2−6] A canonical PDZ domain contains ∼90 amino acids and can bind specifically to a short peptide at the extreme C terminus of target proteins and/or an internal sequence with restrained conformation.[7−10] In addition, recent studies have shown that the PDZ domains also contain lipid binding capability.[11]

In many multiple PDZ domain-containing proteins, PDZ modules are arranged in closely linked groups. Accumulating evidence indicates that tandem PDZ repeats of these proteins show distinct target-binding properties from the individual PDZ domains or from a simple sum of the two PDZ domains in the repeats.[1,12,13] For example, the tandem PDZ domains PDZ12 and PDZ45 of GRIP each form a compact structure with a fixed interdomain orientation, in which one PDZ domain in each of the tandem domain functions to stabilize the structure of the other PDZ.[12,14] In X11α/Mint1, the two tandem PDZ domains together with the entire C terminal tail of the protein form an integral structural unit, and the protein adopts an autoinhibited conformation.[13] In the previous study of the PDZ12 tandem of PSD-95,[1] the two PDZ domains were found to have limited freedom of rotation relative to each other, so that the two peptide-binding grooves of the PDZ tandem are oriented in more or less the same direction. Increasing the spacing between PDZ1 and PDZ2 resulted in decreased binding between PDZ12 and its dimeric targets. It was proposed that this supramodular organization is specialized to facilitate interaction of the PDZ12

† Department of Chemistry, Fudan University.
‡ Institute of Biomedical Sciences, Fudan University.
§ Wuhan Institute of Physics and Mathematics.
|| Hong Kong University of Science and Technology.

(1) Long, J. F.; Tochio, H.; Wang, P.; Fan, J. S.; Sala, C.; Niethammer, M.; Sheng, M.; Zhang, M. J. *J. Mol. Biol.* **2003**, *327*, 203–214.
(2) Zhang, M. J.; Wang, W. N. *Acc. Chem. Res.* **2003**, *36*, 530–538.
(3) Craven, S. E.; Bredt, D. S. *Cell* **1998**, *93*, 495–498.
(4) Fanning, A. S.; Anderson, J. M. *J. Clin. Invest.* **1999**, *103*, 767–772.
(5) Garner, C. C.; Nash, J.; Huganir, R. L. *Trends Cell Biol.* **2000**, *10*, 274–280.
(6) Sheng, M.; Sala, C. *Annu. Rev. Neurosci.* **2001**, *24*, 1–29.
(7) Doyle, D. A.; Lee, A.; Lewis, J.; Kim, E.; Sheng, M.; MacKinnon, R. *Cell* **1996**, *85*, 1067–1076.
(8) Hillier, B. J.; Christopherson, K. S.; Prehoda, K. E.; Bredt, D. S.; Lim, W. A. *Science* **1999**, *284*, 812–815.
(9) Tochio, H.; Zhang, Q.; Mandal, P.; Li, M.; Zhang, M. J. *Nat. Struct. Biol.* **1999**, *6*, 417–421.
(10) Tochio, H.; Mok, Y. K.; Zhang, Q.; Kan, H. M.; Bredt, D. S.; Zhang, M. J. *J. Mol. Biol.* **2000**, *303*, 359–370.
(11) Wu, H.; Feng, W.; Chen, J.; Chan, L. N.; Huang, S. Y.; Zhang, M. J. *Mol. Cell* **2007**, *28*, 886–898.
(12) Feng, W.; Shi, Y. W.; Li, M.; Zhang, M. J. *Nat. Struct. Biol.* **2003**, *10*, 972–978.
(13) Long, J. F.; Feng, W.; Wang, R.; Chan, L. N.; Ip, F. C. F.; Xia, J.; Ip, N. Y.; Zhang, M. J. *Nat. Struct. Mol. Biol.* **2005**, *12*, 722–728.
(14) Long, J. F.; Wei, Z. Y.; Feng, W.; Yu, C.; Zhao, Y. X.; Zhang, M. J. *J. Mol. Biol.* **2008**, *375*, 1457–1468.

tandem to multimeric trans-membrane proteins, such as receptors and ion channels.

To fully understand the target binding property as well as the functional implication of the supramodular nature of the PSD-95 PDZ12 tandem, it is essential to characterize the structure of the tandem in complex with its targets. Elucidation of the PDZ12 dynamics will also help to uncover the molecular basis governing the PDZ12 tandem-mediated target interactions. In this report, we solved the three-dimensional structure of PSD-95 PDZ12 in complex with a binding peptide consisting of the PSD-95 PDZ12 binding motif of cypin. The individual domain structures do not show significant changes upon peptide binding, but the restrained interdomain orientation disappears with concomitant large increases of inter-PDZ mobility. This dramatic change in protein dynamics represents a previously unappreciated property of PSD-95 PDZ12 and perhaps of other tandemly arranged supramodules for encoding their ligand binding affinities and specificities.

Materials and Methods

Cloning, Expression, and Purification of PSD-95 PDZ12. PDZ1, PDZ2, and PDZ12 were PCR-amplified from the full-length rat PSD-95 cDNA using appropriate primers and inserted into the *Xho I* and *Bam HI* sites of the plasmid pET14b, respectively. Expression and purification of the recombinant PDZ domains from BL21(DE3) *E. coli* host cells followed the method described previously.[1] Uniformly $^{15}N/^{13}C$-labeled PDZ domains were prepared by growing the bacteria in an M9 minimal medium using $^{15}NH_4Cl$ as the sole nitrogen source or $^{15}NH_4Cl$ and ^{13}C-labeled glucose as the sole nitrogen and carbon source, respectively. A nine residue peptide (QVVPFSSSV) corresponding to the last nine residues of rat cypin was synthesized commercially. The peptide was purified by reversed phase HPLC.

NMR Experiments. NMR spectra for the determination of the PDZ12/cypin peptide complex structure were acquired at 30 °C on Varian Inova 500 and 750 MHz spectrometers. Sequential backbone and nonexchangeable side-chain resonance assignments of the protein were obtained by standard heteronuclear correlation experiments including HNCO, HNCA, HN(CO)CA, HNCACB, CACB(CO)NH, and HCCH-TOCSY experiments and confirmed by a 3D ^{15}N-separated NOESY experiment.[15,16] The residual dipolar coupling constants of the PDZ12/cypin complex were obtained by recording the in-phase/antiphase (IPAP) $^1H-^{15}N$ HSQC spectra of the protein in the absence and presence of 20% Pf1 phage.[17]

^{15}N T_1, $T_{1\rho}$, and $\{^1H\}$-^{15}N NOE measurements were performed at 30 °C on Bruker Avance III 600 and 800 MHz spectrometers. The T_1 experiments utilized the relaxation delays $T = 10$, 160, 350, 500, 700, 900, 1100 ms for 600 MHz and $T = 10$, 120, 280, 450, 650, 900, 1200 ms for 800 MHz. The relaxation delays used in $T_{1\rho}$ measurements were: 2, 12, 22, 32, 42, 54, 64 ms for 600 MHz and 2, 8, 17, 26, 36, 46, 58 ms for 800 MHz. The recycle delays for ^{15}N T_1 and $T_{1\rho}$ measurements were 1 and 1.5 s for 600 MHz and 1 and 2 s for 800 MHz, respectively. 16 scans per t_1 point were used for acquisition of T_1, and 8 scans for acquisition of $T_{1\rho}$. Relaxation times were determined by fitting the delay dependent peak intensities to an exponential function. T_2 values were calculated from corresponding T_1 and $T_{1\rho}$ as described previously.[18,19] Steady state $^1H-^{15}N$ NOE values were determined by recording spectra with and without ^1H saturation prior to the start of the experiments. The total recycle delays for the NOE measurements were 8.5 and 9 s for 600 and 800 MHz, respectively. A total of 16 transients were collected in NOE measurements.

Structure Calculations. Approximate interproton distance restraints were derived from NOESY spectra (^{15}N-separated NOESY and ^{13}C-separated NOESY). NOEs were grouped into three distance ranges of 1.8−2.7 Å (1.8−2.9 Å for NOEs involving NH protons), 1.8−3.3 Å (1.8−3.5 Å for NOEs involving NH protons), and 1.8−5.0 Å, corresponding to strong, medium, and weak NOEs. Hydrogen bonding restraints were generated from the standard secondary structure of the protein based on NOE patterns and backbone secondary chemical shifts. Backbone dihedral angle restraints were derived from the secondary structure of the protein and backbone chemical shift analysis program TALOS.[20] Structures were calculated using the program CNS.[21] The figures were generated using MOLMOL,[22] MOLSCRIPT,[23] and Raster3D.[24]

Protein Data Bank Accession Number. The coordinates of the structures of the PSD-95 PDZ12/cypin complex have been deposited in the Protein Data Bank under the accession code 2ka9.

NMR Relaxation Data Analysis. For the simple model-free analysis in the frame of isotropic overall motion, the data were fitted to the spectra density of

$$J(\omega) = \left[\frac{S^2\tau_c}{1+(\omega\tau_c)^2} + \frac{(1-S^2)\tau'}{1+(\omega\tau')^2}\right] \quad (1)$$

where $1/\tau' = 1/\tau_c + 1/\tau_e$, τ_c is the overall rotational correlation time, and S^2 is the generalized order parameter characterizing the amplitude of internal motion on the time scale τ_e.

For "extended model-free" analysis with isotropic overall motion, the spectra density is

$$J(\omega) = \frac{S_f^2 S_s^2 \tau_c}{1+(\omega\tau_c)^2} + \frac{S_f^2(1-S_s^2)\tau'}{1+(\omega\tau')^2} \quad (2)$$

where $1/\tau' = 1/\tau_c + 1/\tau_e$, S_f^2 is the order parameter for fast internal motion, and S_s^2 and τ_e characterize the slow internal motion. When overall motion is assumed to be axial asymmetric, the spectra density of the extended model-free method is

$$J(\omega) = \sum_{k=1}^{3} A_k \left\{\frac{S_f^2 S_s^2 \tau_k}{1+(\omega\tau_{e,k})^2} + \frac{S_f^2(1-S_s^2)\tau_{e,k}}{1+(\omega\tau_{e,k})^2}\right\} \quad (3)$$

with

$$A_1 = 0.75\sin^4\alpha,\ A_2 = 3(\sin^2\alpha)(\cos^2\alpha),\ A_3 = (1.5\cos^2\alpha - 0.5)^2$$

$$\tau_1 = (4D_{\|} + 2D_{\perp})^{-1},\ \tau_2 = (D_{\|} + 5D_{\perp})^{-1},\ A_3 = (1.5\cos^2\alpha - 0.5)^2$$

$$\frac{1}{\tau_{e,k}} = \frac{1}{\tau_e} + \frac{1}{\tau_k} \text{ where } k = 1, 2, 3$$

where α is the angle between the N−H bond vector and the long axis of the rotational diffusion tensor and $D_{\|}$ and $D_{\perp}$ are the parallel and perpendicular components of this tensor, respectively. The effective overall correlation time for axially symmetric model is $\tau_{c,eff} = (4D_{\perp} + 2D_{\|})^{-1}$.

(15) Kay, L. E.; Gardner, K. H. *Curr. Opin. Struct. Biol.* **1997**, *7*, 722–731.
(16) Clore, G. M.; Gronenborn, A. M. *Trends Biotechnol.* **1998**, *16*, 22–34.
(17) Ottiger, M.; Delaglio, F.; Bax, A. *J. Magn. Reson.* **1998**, *131*, 373–378.
(18) Davis, D. G.; Perlman, M. E.; London, R. E. *J. Magn. Reson., Ser. B* **1994**, *104*, 266–275.
(19) Tjandra, N.; Wingfield, P.; Stahl, S.; Bax, A. *J. Biomol. NMR* **1996**, *8*, 273–284.
(20) Cornilescu, G.; Delaglio, F.; Bax, A. *J. Biomol. NMR* **1999**, *13*, 289–302.
(21) Brunger, A. T.; Adams, P. D.; Clore, G. M.; DeLano, W. L.; Gros, P.; Grosse-Kunstleve, R. W.; Jiang, J. S.; Kuszewski, J.; Nilges, M.; Pannu, N. S.; Read, R. J.; Rice, L. M.; Simonson, T.; Warren, G. L. *Acta Crystallogr. D* **1998**, *54*, 905–921.
(22) Koradi, R.; Billeter, M.; Wuthrich, K. *J. Mol. Graphics Modell.* **1996**, *14*, 51–55.
(23) Kraulis, P. J. *J. Appl. Crystallogr.* **1991**, *24*, 946–950.
(24) Merritt, E. A.; Murphy, M. E. P. *Acta Crystallogr., Sect. D* **1994**, *50*, 869–873.

Following the analysis method proposed in ref 25, relaxation data of each residue were fitted to the spectra density function separately:

$$J(\omega) = \left[\frac{S^2 \tau_c}{1 + (\omega \tau_c)^2} + \frac{(1 - S^2)\tau_e}{1 + (\omega \tau_e)^2} \right] \quad (4)$$

The parameters which best reproduce the data correspond to a global minimum in the error. The target function used is defined as

$$\chi^2 = \sum_{i=1}^{N} \sum_{j=1}^{M} \left\{ \frac{(R_{1ij} - \hat{R}_{1ij})^2}{\sigma^2_{R_1 ij}} + \frac{(R_{2ij} - \hat{R}_{2ij})^2}{\sigma^2_{R_2 ij}} + \frac{(NOE_{ij} - N\hat{O}E_{ij})^2}{\sigma^2_{NOEij}} \right\} \quad (5)$$

Program ModelFree 4.20[26] and an in-house written program were used in the calculations.

Molecular Dynamics Simulation. All the molecular dynamics simulations were carried out using the program GROMACS v3.2.1 (http://www.gromacs.org) with an OPLS/AA force field.[27−29] All starting structures were solvated with Simple Point Charge water molecules.[30] Temperature was maintained at 300 K using the Berendsen thermostat[31] with a coupling constant of 0.1 ps, and the system pressure was maintained at 1 bar using the Berendsen barostat[31] with a coupling constant of 0.5 ps and compressibility of 4.5×10^{-5} bar^{-1}. Long-range electrostatic interactions were estimated using the Particle Mesh Ewald method[32] with a cutoff of 1.0 Å. Bonds were constrained using the algorithm LINCS[33] for protein and SETTLE[34] for water. Each system was energy minimized followed by a 100 ps equilibrium run with non-hydrogen atoms harmonically restrained with a force constant of 1000 kJ/mol/Å. All restraints were then removed, and the production run for each system was 12 ns.

The domain orientation was defined by a vector pointing from the center of mass of each PDZ domain (MCdmn) to the center of mass of the three very C terminal amino acids of the bound cypin peptide (MCpep). Based on this, Θ was defined as the angle between the two domain orientation vectors of PDZ1 and PDZ2, respectively. And a dihedral angle Φ was defined by the two domain orientation vectors connected at the centers of mass of PDZ1 and PDZ2, i.e., the dihedral angle of MCpep1-MCdmn1- MCdmn2-MCpep2.

Results and Discussion

Solution Structure of the PDZ12/Cypin Complex. PSD-95 PDZ12 protein (referred to as PDZ12 from hereafter) was titrated with synthetic peptide corresponding to the last nine residues of rat cypin (QVVPFSSSV)[35] by recording a series of ^{1}H−^{15}N HSQC spectra. The peaks of PDZ1 and PDZ2 shifted simultaneously upon peptide addition, and the titration curves indicate that the cypin peptide binds to PDZ1 and PDZ2 with similar affinities (data not shown).

Conventional heteronuclear multidimensional NMR spectroscopic techniques were used to determine the solution structure of the PDZ12/cypin peptide complex. Since no interdomain NOEs were found in the NOESY spectra of the PDZ12/cypin complex, the interdomain orientation was not fixed in the NMR-derived structures. In Figure 1, the structure of the PDZ12/cypin complex is presented with two separate parts, each representing PDZ1 and PDZ2 in complex with the cypin peptide, respectively. Both PDZ1 and PDZ2 adopt the canonical PDZ domain fold as expected, and there are no significant structural changes upon ligand binding with respect to the free form PDZ1 or PDZ2. Superposition of the backbone atoms of the free and the complex forms gives rise to root-mean-square-deviation (rmsd) values of 1.75 Å for PDZ1 and 1.45 Å for PDZ2 domains. The cypin peptide binds to the canonical binding groove between αB and βB in both PDZ1 and PDZ2. The C-terminal three residues ("SSV") of the cypin peptide are well-defined. The side chain of Val 0 at the very C-terminus of the cypin peptide is situated into a hydrophobic pocket comprised of several highly conserved hydrophobic amino acids, including Leu75, Phe77, and Leu137 in PDZ1 and Leu170, Phe172, and Leu232 in PDZ2. It is well established that in the class I PDZ domains the His residue at the αB1 selects for Ser or Thr at the −2 position of ligand peptides.[2] Here, the side chains of both His130 in PDZ1 and His225 in PDZ2 are in close proximity with the hydroxyl group from the side chain of the −2 Ser of the cypin peptide.

The interaction between the cypin peptide and PDZ12 was also examined with backbone chemical shift perturbations. The ^{15}N−^{1}H HSQC spectra of free form PDZ12 and PDZ12−cypin complex were compared, and significant chemical shift changes were found (data not shown). Since these chemical shift changes may have resulted from the protein−peptide interaction as well as a possible interdomain conformational change upon ligand binding, we compared the ^{15}N−^{1}H HSQC spectra of the isolated PDZ1 (or PDZ2) and PDZ1 (or PDZ2) in complex with the cypin peptide to probe the chemical shift changes of the two PDZ domains solely originated from the cypin peptide binding. The cypin peptide-induced chemical shift perturbation patterns of PDZ1 and PDZ2 are similar (Figure 2). The peptide-binding-induced chemical shift changes are most obvious at the ligand binding groove of each PDZ (i.e., αB, βB, and the GLGF loop). The chemical shift perturbation patterns of both PDZ1 and PDZ2 are very similar to that of PDZ2 upon binding to the CAPON peptide.[36] It is interesting to note that residues from the αA in both PDZ domains also experience large chemical shift changes even though these residues are located away from the binding site. This long-range interaction in PDZ domains was predicted and experimentally probed.[37]

To examine possible interdomain interaction in the PDZ12/cypin complex, we compared its ^{1}H−^{15}N HSQC spectrum with those of the isolated PDZ1/cypin and PDZ2/cypin complexes. The three superimposed spectra shown in Figure S1 indicate that the summation spectrum of the isolated PDZ1/cypin and PDZ2/cypin complexes is strikingly similar to the spectrum of

(25) Yang, D. W.; Mok, Y. K.; FormanKay, J. D.; Farrow, N. A.; Kay, L. E. *J. Mol. Biol.* **1997**, *272*, 790–804.
(26) Mandel, A. M.; Akke, M.; Palmer, A. G. *J. Mol. Biol.* **1995**, *246*, 144–163.
(27) Berendsen, H. J. C.; Vanderspoel, D.; Vandrunen, R. *Comput. Phys. Commun.* **1995**, *91*, 43–56.
(28) Lindahl, E.; Hess, B.; van der Spoel, D. *J. Mol. Model.* **2001**, *7*, 306–317.
(29) Van der Spoel, D.; Lindahl, E.; Hess, B.; Groenhof, G.; Mark, A. E.; Berendsen, H. J. C. *J. Comput. Chem.* **2005**, *26*, 1701–1718.
(30) Hermans, J.; Berendsen, H. J. C.; van Gunsteren, W. F.; Postma, J. P. M. *Biopolymers* **1984**, *23*, 1513–1518.
(31) Berendsen, H. J. C.; Postma, J. P. M.; van Gunsteren, W. F.; DiNola, A.; Haak, J. R. *J. Chem. Phys.* **1984**, *81*, 3684–3690.
(32) Darden, T.; York, D.; Pedersen, L. *J. Chem. Phys.* **1993**, *98*, 10089–10092.
(33) Hess, B.; Bekker, H.; Berendsen, H. J. C.; Fraaije, J. *J. Comput. Chem.* **1997**, *18*, 1463–1472.
(34) Miyamoto, S.; Kollman, P. A. *J. Comput. Chem.* **1992**, *13*, 952–962.
(35) Firestein, B. L.; Brenman, J. E.; Aoki, C.; Sanchez-Perez, A. M.; El-Husseini, A. E. D.; Bredt, D. S. *Neuron* **1999**, *24*, 659–672.
(36) Tochio, H.; Hung, F.; Li, M.; Bredt, D. S.; Zhang, M. J. *J. Mol. Biol.* **2000**, *295*, 225–237.
(37) Lockless, S. W.; Ranganathan, R. *Science* **1999**, *286*, 295–299.

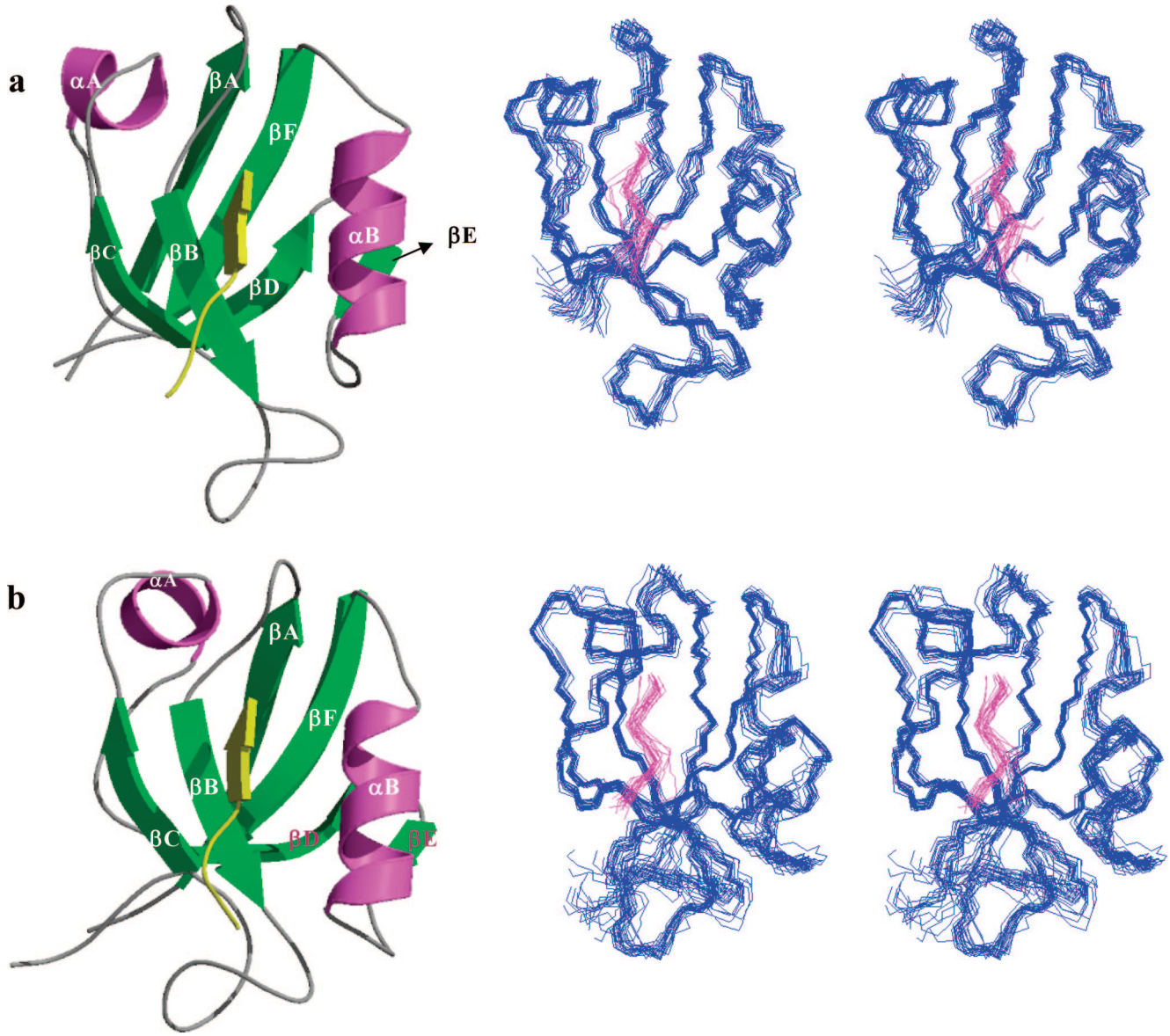

Figure 1. Solution structure of the PDZ12/cypin peptide complex. Ribbon diagram and stereoview of PDZ1 (a) and PDZ2 (b) domains in the PDZ12/cypin complex. The cypin peptide is drawn in yellow. The stereoview diagrams show the best-fit superposition of the backbone atoms of the PDZ1 or PDZ2 from the final 20 structures of the PDZ12/cypin complex. Due to the interdomain flexibility, the two PDZ structures are presented separately.

the PDZ12/cypin complex. The residues that experience large chemical shift difference in the above comparison are located either at the C-terminal end of PDZ1 or at the N-terminus of PDZ2 domains (Figure S1b). The C terminal of PDZ1 and N terminal of PDZ2 flanking the PDZ12 linker are expected to have large chemical shift changes in the above comparison as this region is covalently joined together in the PDZ12 tandem. This is in sharp contrast to the case of free form PDZ12, where significant chemical shift differences were observed for many residues in the internal regions of PDZ1 and PDZ2 when comparing the HSQC spectra of isolated PDZ1 and PDZ2 with that of PDZ12, indicating direct domain−domain interactions.[1] Therefore, both the chemical shift perturbation experiment and the lack of interdomain NOEs indicate that the two PDZ domains in the PDZ12/cypin peptide complex lack direct interdomain interactions. In the free form of the PDZ12 tandem, the conformational flexibility is limited and the two PDZs have relatively fixed domain orientations.[1] The loss of interdomain contact in the PDZ12/cypin complex, however, does not necessarily mean that the interdomain orientation is also lost. Both the time scales and the time-averaged properties of NMR chemical shifts as well as NOEs are not sufficient to define the domain orientations and to characterize dynamic properties of the PDZ12/cypin complex.

Characterization of the Interdomain Orientation with Residual Dipolar Coupling Constants. To better characterize the interdomain orientation of the PDZ12/cypin complex, we measured the backbone $^{1}H-^{15}N$ residual dipolar couplings (RDCs) by dissolving the protein complex in a nematic phase of negatively charged rod-shaped phage particles. The distribution of the backbone $^{1}H-^{15}N$ RDCs for the two domains of the PDZ12/cypin complex are shown in Figure 3. The distribution patterns of the histograms for PDZ1 and PDZ2 are quite different. The magnitude of the alignment tensor was determined from the maximum, minimum, and mode of the distribution as reported.[38] The axial component (D_a^{NH}) of the alignment tensor and the rhombicity η (D_r/D_a) for the PDZ1 domain is 15.7 Hz and 0.28, while those for the PDZ2 domain are 11.9 Hz and

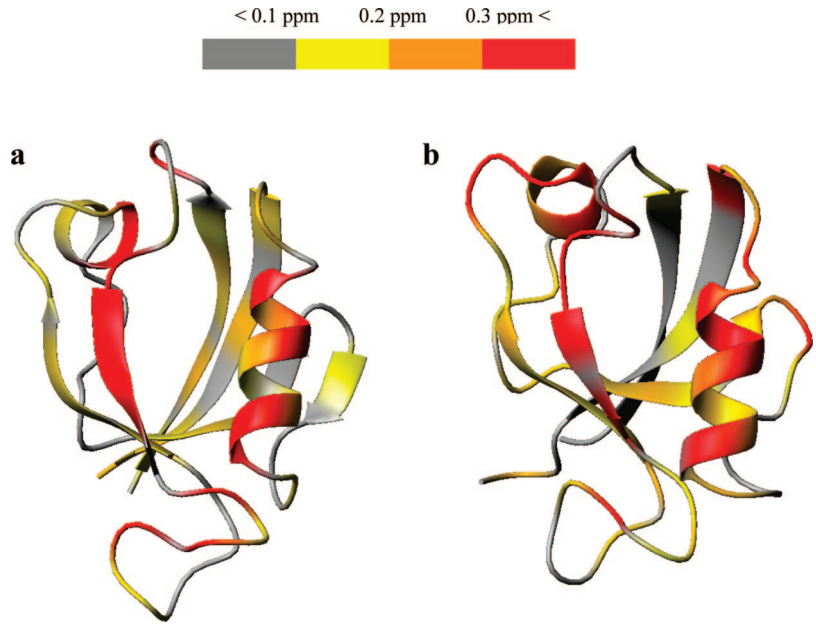

Figure 2. Mapping of the cypin peptide-binding induced chemical shift changes onto the three-dimensional structure of (a) PDZ1 and (b) PDZ2. The combined ^{1}H and ^{15}N chemical shift changes are defined as $\Delta ppm = [(\Delta\delta_{HN})^2 + (\Delta\delta_N \times \alpha_N)^2]^{1/2}$, where $\Delta\delta_{HN}$ and $\Delta\delta_N$ represent the chemical shift difference. The scaling factor α_N to normalize the ^{1}H and ^{15}N chemical shifts is 0.20.

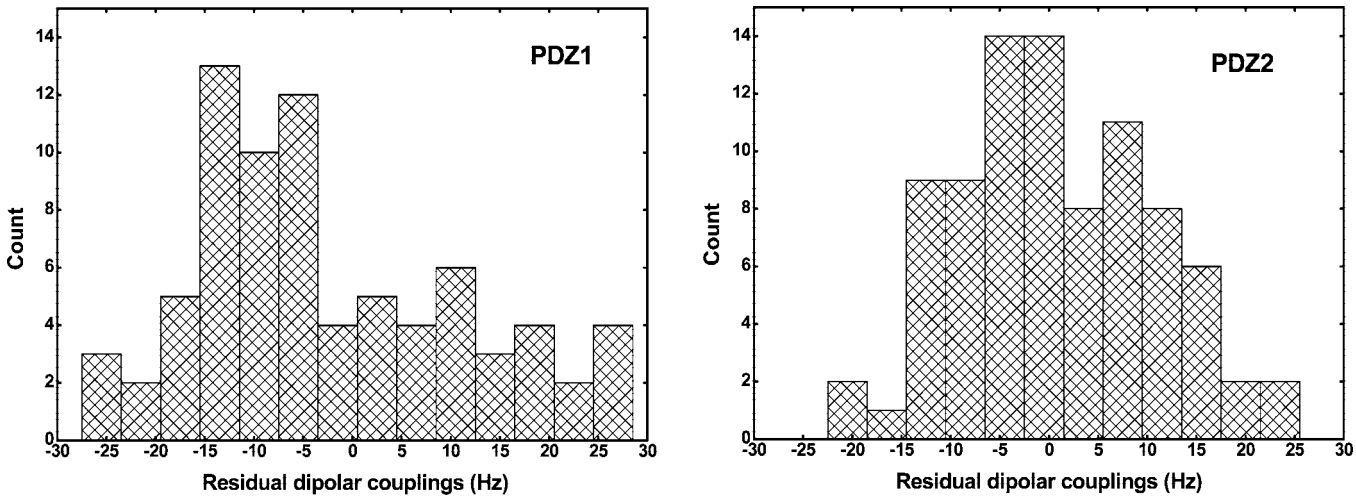

Figure 3. Histograms of the backbone $^{1}H-^{15}N$ residual dipolar couplings of PDZ12 in complex with the cypin peptide. The obviously different distribution patterns of RDC values between PDZ1 and PDZ2 indicate that interdomain orientation is not defined.

0.46, respectively. If the PDZ12 complex was rigid with minimal interdomain motion as in the case of the free form PDZ12, dipolar couplings measured for both PDZ domains would be described by a single alignment tensor; i.e., the magnitude of the alignment tensor and rhombicity would be identical or at least highly similar. The significant differences of both the magnitude of the alignment tensor and the rhombicity thus indicate that the two PDZ domains are aligned independently or semi-independently resulting from the interdomain motion.[39] The alignment tensor for each domain could be affected by its size, shape, and electrostatic properties in charged liquid crystalline media such as the phages used here. Since the size and shape of PDZ1 and PDZ2 are very similar, the difference in alignment tensor could be accounted for by the different surface charges of PDZ1 and PDZ2. Although the RDCs gave clear indication of interdomain motion, they do not provide information for the time scale and magnitude of the motion. So we further explored the protein dynamics from analysis of NMR relaxation data.

Analysis of Interdomain Motion by NMR-Based Relaxation Studies. ^{15}N relaxation data T_1, T_2, and $^{15}N-^{1}H$ NOE of PDZ12/cypin complex were measured at 30 °C under two field strengths of 600 and 800 MHz. At a glance, we find that the values of longitudinal relaxation time T_1 at the PDZ1 region are larger than those of PDZ2 and the T_2 values of PDZ1 are smaller than those of PDZ2 accordingly (Figure 4). As the T_1/T_2 ratio is, to a first approximation, a measure of the global rotational correlation time τ_c, we can roughly estimate that PDZ1 has a larger τ_c than PDZ2. The low values of $^{15}N-^{1}H$ NOE at the linker region between PDZ1 and PDZ2 indicate the flexible

(38) Clore, G. M.; Gronenborn, A. M.; Bax, A. *J. Magn. Reson.* **1998**, *133*, 216–221.
(39) Braddock, D. T.; Cai, M. L.; Baber, J. L.; Huang, Y.; Clore, G. M. *J. Am. Chem. Soc.* **2001**, *123*, 8634–8635.

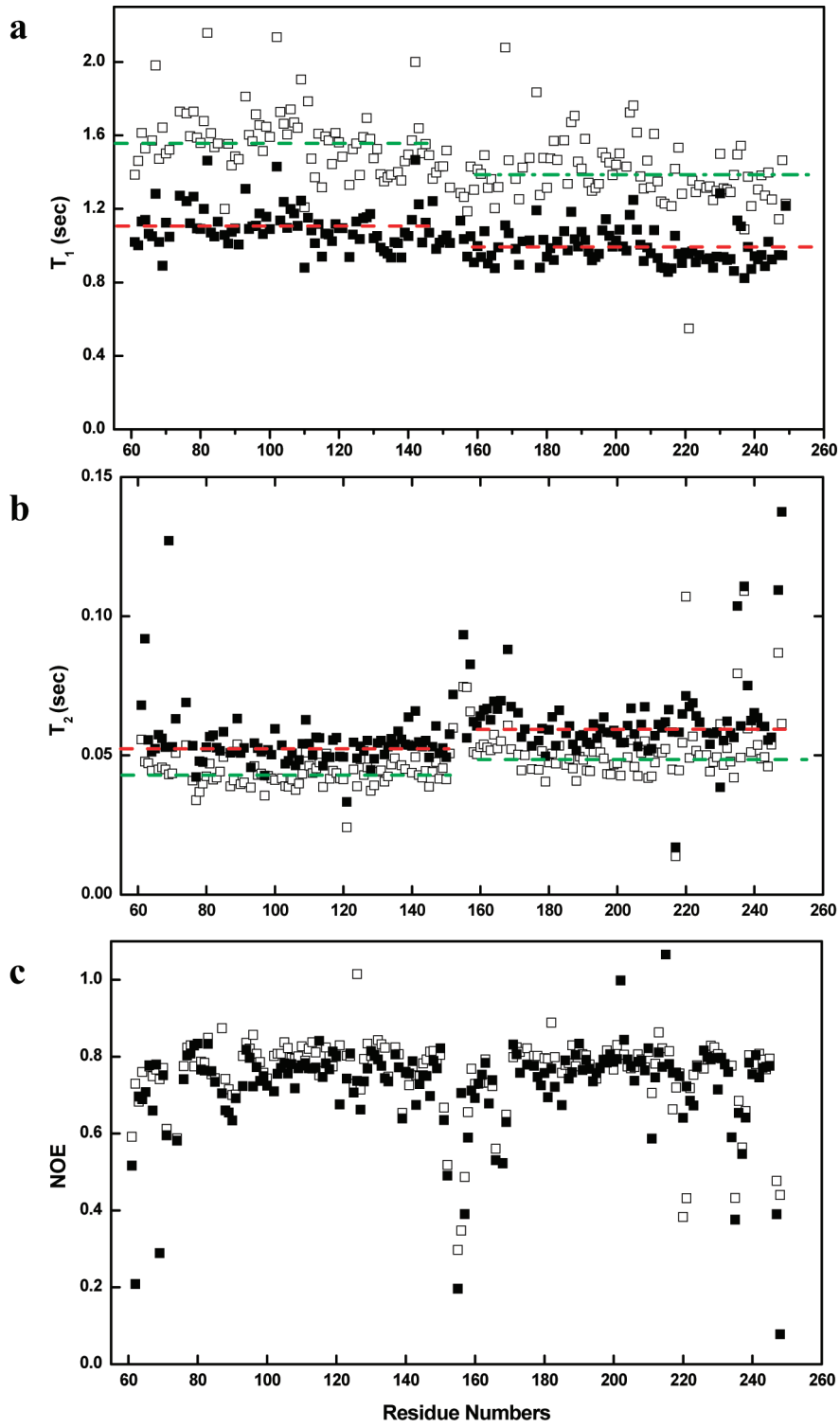

Figure 4. ^{15}N relaxation data, T_1 (a), T_2 (b), and ^{1}H−^{15}N NOE (c), for the PDZ12/cypin complex measured at 30 °C and at ^{1}H frequencies of 600 MHz (■) and 800 MHz (□). Horizontal dashed lines denote the average values of T_1 and T_2 for PDZ1 or PDZ2 domains under the field strength of 600 MHz (red) and 800 MHz (green), respectively.

nature of the linker. First, the T_1, T_2, and NOE data are analyzed following the conventional "model-free"[40] and "extended model-free" methods[41] assuming isotropic overall rotation of the protein, and the overall rotational correlation time τ_c was determined globally. In the simple model-free analysis, the fit errors are large and beyond the confidence limit for most of the residues (Table S1). For many residues, the correlation time of internal motions τ_e are exceptionally slow, indicating that the simple model-free approach is not applicable and additional motions must be considered in addition to the usual fast backbone vibration motions. When data from two fields are fitted simultaneously, the fit errors further increased. The "extended model-free" analysis[41] that incorporates two order parameters to account for internal motions at two time scales gave reduced

(40) Lipari, G.; Szabo, A. *J. Am. Chem. Soc.* **1982**, *104*, 4546.

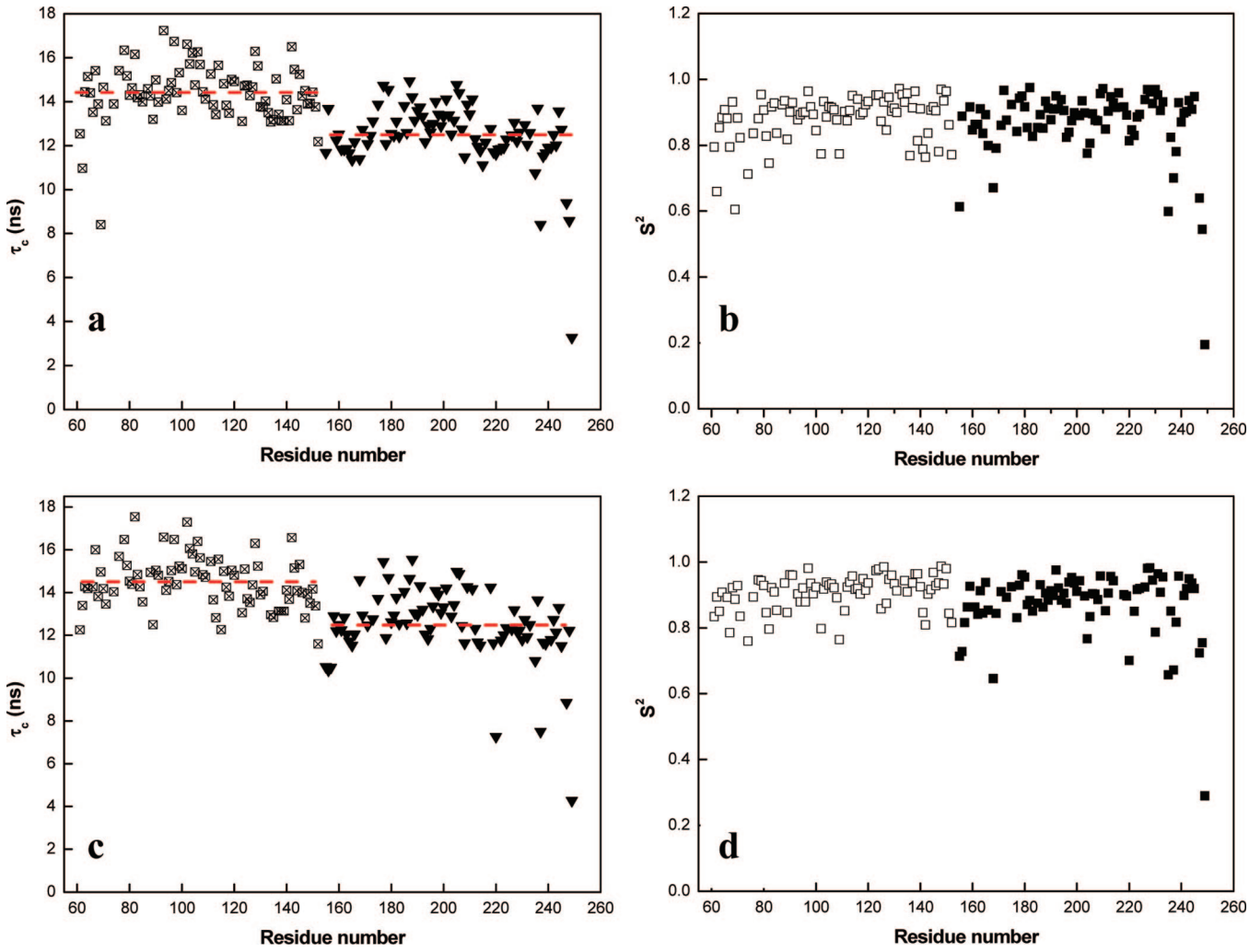

Figure 5. Overall rotational correlation time τ_c extracted at per residue basis for PDZ1 (square) and PDZ2 (triangle) using the data measured at ^{1}H frequencies of 600 MHz (a) and 800 MHz (c). Horizontal dashed lines denote the average values of τ_c. Order parameters S^2 of PDZ1 (□) and PDZ2 (■) calculated using the data measured at ^{1}H frequencies of 600 MHz (b) and 800 MHz (d).

fit errors compared with the simple model-free method (Table S1). However, the fitting errors for many residues are still too large to fall in the acceptable confidence limit. The order parameters S_s^2 associated with the slow motion are not reasonably determined, since most of them are larger than the order parameters S_f^2 characterizing fast motions, indicating the inadequacy of the extended model-free method. Incorporating the effect of anisotropic rotational motion by using the axially symmetric rotational diffusion model combined with the two time scale extended model-free approach does not improve the fitting (Table S1), as the fitting errors are almost the same as those of the isotropic model.

The basic assumption of the model-free method is that the overall rotational motion of the protein and the internal motions are statistically independent of each other. The justification of this assumption is the significant difference of the characteristic time scales of these motions. In the case of the PDZ12/cypin complex, however, this approximation may not be valid. The interdomain motions may strongly couple with the overall rotational motion and, thus, could significantly change the shape of the whole protein. In such a flexible system, it is likely that there exists a distribution of molecular shapes. Therefore, the concept of a time independent rotational diffusion tensor is not applicable anymore. Rigorous treatment of such a system is extremely difficult. However, in the previous study of anisotropic and unfolded proteins, Yang et al.[25] revealed that the order parameters obtained by fitting the relaxation data to the simple model-free spectral density functions in a per residue manner are physically meaningful provided that values of τ_e do not exceed 0.3 ns. The τ_c of each residue thus extracted represents a weighted average of different anisotropic overall motions, while the values of τ_e can not be accurately estimated.

The relaxation data were subjected to such analysis and the extracted τ_c and S^2 are presented in Figure 5. The results with τ_e longer than 0.3 ns were excluded due to the poor reliability. The two PDZ domains obviously have different values of τ_c (Figure 5a, c). At a field strength of 600 MHz, the average value of τ_c is 14.4 ns for PDZ1 and 12.5 ns for PDZ2. The data measured at 800 MHz field strength gave very similar results. The significant difference in τ_c between the two domains is consistent with the observations of the raw T_1 and T_2 data, indicating the existence of slow interdomain motions. In an extreme situation where the two PDZ domains have totally fixed orientations and tumble as a single rigid body in solution, the

(41) Clore, G. M.; Szabo, A.; Bax, A.; Kay, L. E.; Driscoll, P. C.; Gronenborn, A. M. *J. Am. Chem. Soc.* **1990**, *112*, 4989–4991.

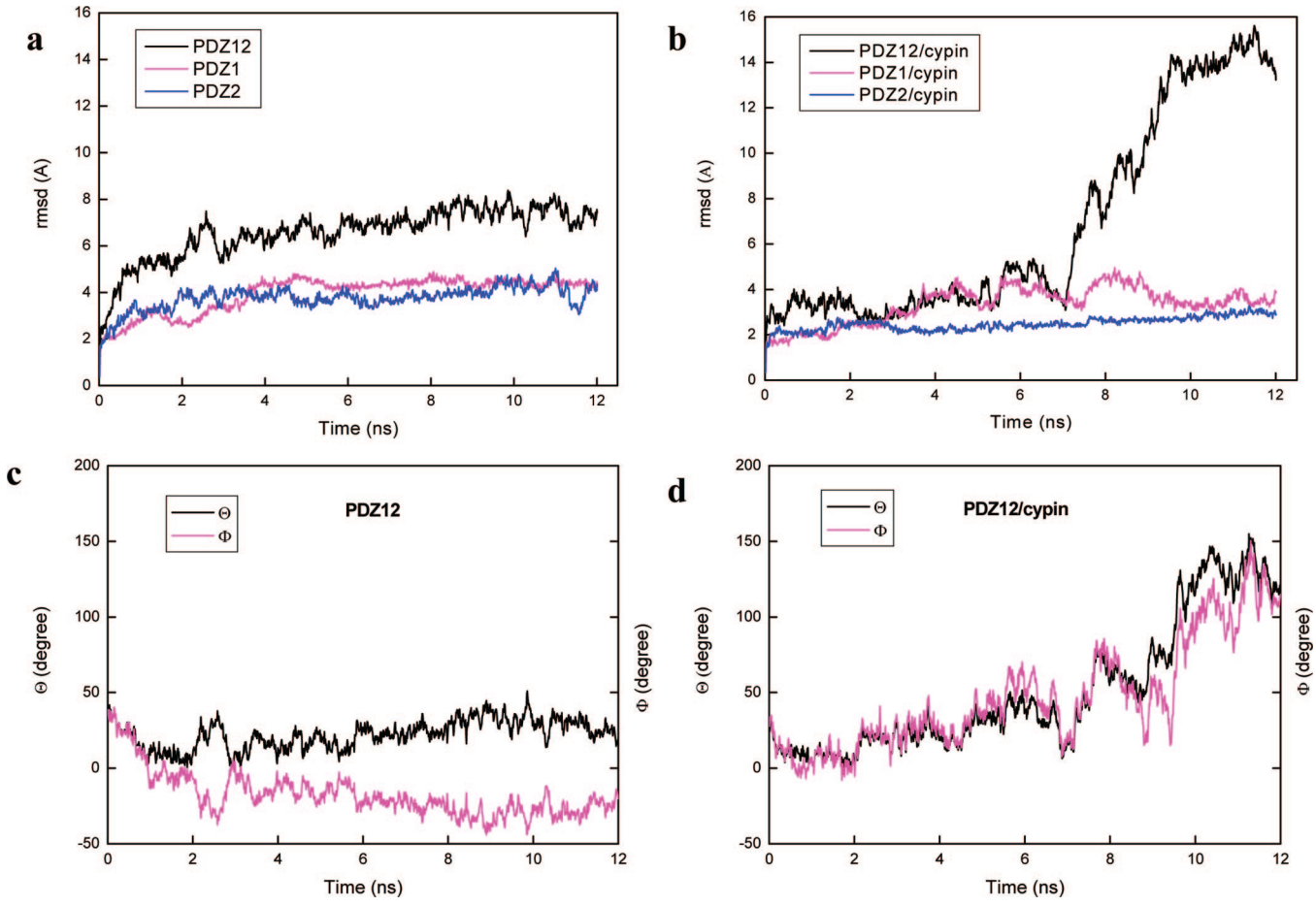

Figure 6. Evolutions of the root-mean-square deviations (rmsd) of C_α atoms and angle Θ and dihedral angle Φ with respect to the starting structures in the MD simulations. (a) The rmsd of the whole protein (black), PDZ1 (magenta), and PDZ2 (blue) of the ligand-free PDZ12. (b) The rmsd of the whole protein (black), PDZ1 (magenta), and PDZ2 (blue) of the PDZ12/cypin complex. (c) Evolution of the angles for the ligand-free PDZ12. (d) Evolution of the angles for the PDZ12/cypin complex.

overall correlation time τ_c for PDZ1 and PDZ2 should be the same. In another extreme where each PDZ domain rotates freely like two beads on a string, the correlation time for PDZ1 and PDZ2 will be the same as those of individual isolated PDZ domains. The analysis of NMR relaxation data of the isolated PSD95 PDZ2 gives an overall correlation time of 6.04 ns.[36] The dynamic property of the PDZ12/cypin peptide complex should be between the two extreme situations. The order parameter S^2 shown in Figure 5b and 5d demonstrates typical backbone flexibilities of folded proteins. In the previous study of the PSD-95 PDZ2 domain,[36] backbone dynamics were also examined by NMR relaxation experiments. The order parameters extracted from conventional model-free analysis are very similar with the values obtained in this work of the PDZ2 region in the PDZ12/cypin complex, except for the residues in the GLGF loops that are directly involved in peptide binding. A detailed and quantitative comparison of the backbone order parameters between isolated PDZ2 and the PDZ12/cypin complex is not applicable, since the order parameters derived here for PDZ12/cypin is less accurate than those of the isolated PDZ2. Since the values of order parameters describe the amplitude of local bond vector motions, the results shown in Figure 5b, d are expected for the well-folded proteins and also consistent with the structure of the PDZ12/cypin peptide complex. Although the time scale of relative interdomain motion between PDZ1 and PDZ2 is difficult to estimate in this analysis due to the poor reliability of τ_e values, it was nevertheless clear that there exist slow internal motions with a time scale comparable to the overall rotational motion of the whole protein.

Molecular Dynamics Simulation. The analysis of both the residual dipolar coupling and ^{15}N NMR relaxation data indicate that the PDZ12/cypin complex has significant interdomain motions. However, due to the breakdown of the model-free method, rigorous analysis of the NMR relaxation data of this system was not feasible. It is desirable to examine the dynamics of the ligand-free PDZ12 experimentally as well. Unfortunately, the poor behavior of the free form protein (poor peak homogeneity and disappearance of significant amount of backbone amide peaks) prevented us from pursuing detailed NMR relaxation experiments. Therefore we resorted to molecular dynamics (MD) simulations to probe and compare the dynamic behaviors of the ligand-free and -bound forms of PDZ12.

Unrestrained molecular dynamics simulations were performed for the ligand-free PDZ12 and the PDZ12/cypin complex. For free form PDZ12, the model structure with constrained interdomain orientation constructed previously[1] was used as the starting structure. For the PDZ12/cypin complex, the initial structure was built by manually aligning the domain orientation similar with that of the free form PDZ12. Two independent simulations of 12 ns were performed for both systems. The C_α root-mean-square deviations (rmsd) relative to the initial structure as a function of time are presented in Figure 6. It shows that the structures of the individual PDZ domains are essentially stable througout the simulations. After equilibriums were

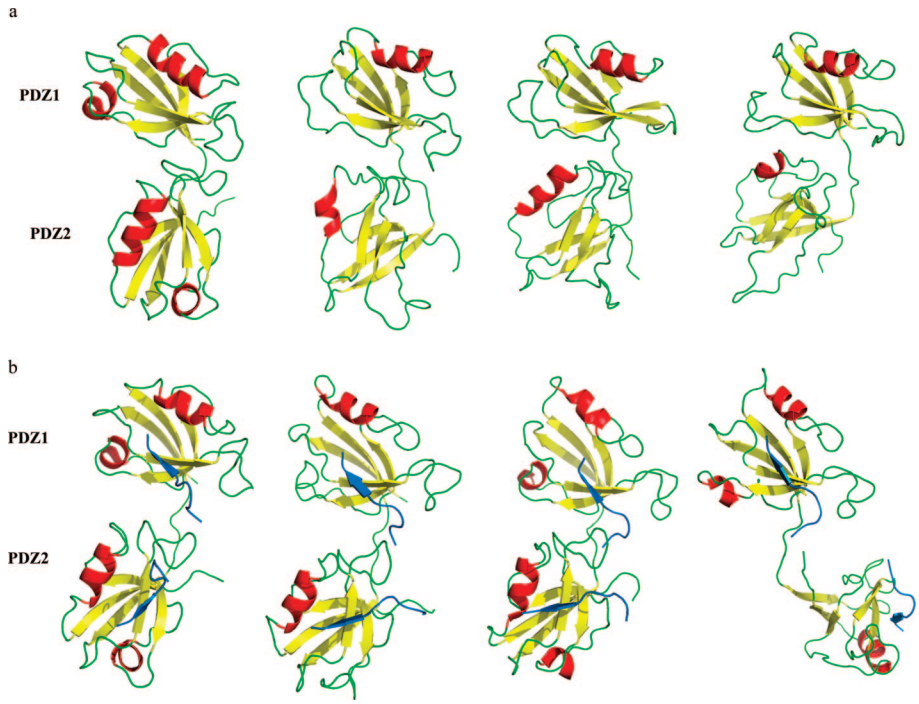

Figure 7. Snapshots of the structures taken from the MD simulation trajectories for (a) the ligand-free form PDZ12 and (b) the PDZ12/cypin complex at 0, 3, 7, and 12 ns, respectively. Cypin peptides bound to PDZ1 and PDZ2 domains are shown in blue.

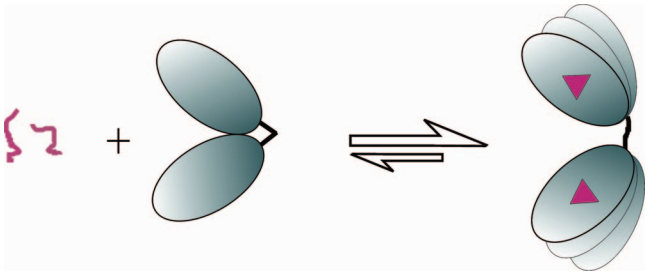

Figure 8. A schematic diagram showing that the two domain protein creates conformational entropy by increasing the interdomain mobility to facilitate the ligand binding. Protein domains are shown as ellipsoids. Free and bound ligand peptides are shown as magenta lines and triangles, respectively.

reached in the simulation systems, the rmsd of individual PDZ domains in the peptide-free protein is slightly larger than those in the peptide bound proteins. Snapshots taken from the trajectories demonstrated transient instabilities of secondary structures in free PDZ12, while the secondary structures in the PDZ12/cypin complex were more stable (Figure 7), indicating that the domain structures are somewhat rigidified upon complex formation. On the other hand, the rmsd value of the whole protein is much larger than those of the individual domains in both lignad-free and -bound forms of PDZ12, indicating pronounced interdomain mobility. However, the conformational flexibilities are remarkably different in the free and the peptide bound PDZ12. Along the trajectory, the rmsd of peptide-free PDZ12 increases gently and reaches equilibrium after 8 ns, fluctuating around the value 7.8 Å. There is no dramatic conformational change during all the simulation time. In contrast, the trajectory of the PDZ12/cypin complex gives rise to a dramatic rmsd increase after 7 ns, and the system has not reached equilibrium even at the end of the simulation at 12 ns. By examining the snapshots taken from the trajectories, it is obvious that the sudden increase of rmsd in the PDZ12/cypin complex corresponds to large conformational changes that alter the relative orientation of the two PDZ domains significantly (Figure 7).

To monitor the conformational change more rigorously, two angles were defined to describe the relative domain orientation (see Materials and Methods). Figure 6c and 6d show the evolution of angle Θ and dihedral angle Φ along the trajectory. Obviously, in the free form PDZ12 the conformational change was limited with Θ and Φ fluctuating in a small range, thereby confining the interdomain conformation in an energy well near the initial conformation. For the peptide-bound system, however, both angles varied in a larger range of values and increased significantly after 7 ns, indicating that the interdomain orientation was not restrained and the protein sampled a much larger conformational space than the free form.

As the initial interdomain orientation of the PDZ12/cypin complex is manually aligned according to the free PDZ12 conformation, one may argue that the artifacts were introduced in the initial model building. Therefore we randomly chose three PDZ12/cypin structures from the NMR-derived structure ensemble and subjected them to MD simulations of 12 ns for each. These experimental structures have quite different conformations representing a few arbitrary interdomain orientations. The resulting trajectories of these simulations demonstrate that all three systems have significant conformational flexibility and show no definite domain orientations throughout the simulations. Along the three trajectories, the initial conformations change dramatically after 4, 6, and 8.5 ns respectively (data not shown). Overall, the molecular dynamics simulations of both the free and peptide-bound forms of PDZ12 clearly show that their dynamic properties are remarkably different. The conformational flexibility of the PDZ12 tandem increases dramatically upon peptide binding by losing the relative interdomain orientation.

It is well-known that protein dynamics plays a key role in protein−ligand interactions which can be characterized by combined contributions of enthalpy and entropy changes during

Table 1. Structural Statistics for the Family of 20 Structures of PDZ12/Cypin Complex[a]

	PDZ12	
distance restraints		
intraresidue ($i - j = 0$)	1294	
sequential ($\|i - j\| = 1$)	777	
medium range ($2 < \|i - j\| < 4$)	415	
long range ($\|I - j\| > 5$)	1005	
hydrogen bonds	30	
total	3520	
dihedral angle restraints		
Φ	100	
Ψ	104	
total	204	
mean rms deviations from experimental restraints		
distance (Å)	0.015 ± 0.001	
dihedral angle (deg)	0.39 ± 0.02	
mean rms deviations for idealized covalent geometry		
bond (Å)	0.0022 ± 0.0001	
angle (deg)	0.38 ± 0.01	
improper (deg)	0.26 ± 0.01	
mean energies (kcal mol^{-1})		
E_{NOE}[b]	57.7 ± 3.76	
E_{cdih}[b]	1.81 ± 0.19	
$E_{L\text{-}J}$	-433.28 ± 14.91	
Ramachandran plot (%)[c]		
most favorable regions	68.0	
additional allowed regions	27.2	
generously allowed regions	3.6	
atomic rms differences (Å)[d]	PDZ1	PDZ2
secondary structure		
backbone heavy atoms	0.49	0.49
all heavy atoms	1.01	0.98

[a] None of the structures exhibits distance violations greater than 0.2 Å or dihedral angle violations greater than 2°. [b] The final values of the square-well NOE and dihedral angle potentials were calculated with force constants of 50 kcal mol^{-1} Å^{-2} and 200 kcal mol^{-1} rad^{-2}, respectively. [c] The program PROCHECK was used to assess the overall quality of the structures. [d] The precision of the atomic coordinates is defined as the average rmd difference between the 20 final structures and the mean coordinates of the protein.

binding reactions. In the "induced-fit" model of ligand binding, many protein dynamics studies gave a conventional scenario in which the backbone flexibility is reduced in a fast time scale to optimize the interaction between protein and ligand.[42] However, significant increases in the backbone or side-chain flexibility upon ligand binding were also observed at specific regions of proteins.[43−45] More generally, it seems that there is a redistribution of the protein dynamics across the protein; i.e., some specific groups experience rigidification while others gain flexibility.[46−48] In the case of PDZ12, however, the dynamics variation upon ligand binding represents a new mode of "induced-fit" effect by changing the interdomain mobility in addition to the local induced fit within an individual domain. By utilizing this domain cooperativity, PDZ12 gains extra compensatory conformational entropy favoring its target binding (Figure 8). We anticipate that this may be one of the general strategies adopted by multidomain scaffold proteins to facilitate its target recognition.

Summary

In the previous work,[1] it was established that the two N-terminal PDZ domains of PDS-95 form a supramodular structure with a restrained domain orientation to facilitate the synergistic target binding. Here, the structural and dynamics studies of the PDZ12/cypin complex revealed another side of the target binding strategy of this PDZ tandem. The restrained domain orientation is lost upon ligand binding, resulting in a significant increase in the interdomain mobility. This change of protein dynamics apparently creates extra conformational entropy, thereby enhancing the binding affinity. The comprehensive understanding of the regulation in ligand binding of PSD-95-PDZ12 may also provide insights into designing inhibitory compounds targeting the PSD-95 PDZ12 tandem for potential stroke therapy.[49]

Acknowledgment. This work was supported by NSFC (No. 20473019), the National High Technology Research Program of China (2006AA02A320), the National Major Basic Research Program of China (2009CB918600), the Shanghai Leading Academic Discipline Project (B108), and the Research Grants Council of Hong Kong. We are grateful to the Shanghai Supercomputer Center and the Fudan University Computer Center for their allocations of computer time. We thank Dr. J. Long for sample preparations, Dr. H. Tochio for the initial spectra analysis, and Dr. D. Yang for insightful discussions and critical comments of the manuscript.

Supporting Information Available: A figure of HSQC spectra and chemical shift changes showing lack of interdomain interaction in PDZ12/cypin complex; a table of the results of conventional model-free and extended model-free analysis. This material is available free of charge via the Internet at http://pubs.acs.org.

JA8076022

(42) Jarymowycz, V. A.; Stone, M. J. *Chem. Rev.* **2006**, *106*, 1624–1671.
(43) Fushman, D.; Ohlenschlager, O.; Ruterjans, H. *J. Biomol. Struct. Dyn.* **1994**, *11*, 1377–1402.
(44) Chi, Y. H.; Kumar, T. K. S.; Chiu, I. M.; Yu, C. *J. Biol. Chem.* **2000**, *275*, 39444–39450.
(45) Sahu, S. C.; Bhuyan, A. K.; Udgaonkar, J. B.; Hosur, R. V. *J. Biomol. NMR* **2000**, *18*, 107–118.
(46) Lee, A. L.; Kinnear, S. A.; Wand, A. J. *Nat. Struct. Biol.* **2000**, *7*, 72–77.
(47) Frederick, K. K.; Kranz, J. K.; Wand, A. J. *Biochemistry* **2006**, *45*, 9841–9848.
(48) Frederick, K. K.; Marlow, M. S.; Valentine, K. G.; Wand, A. J. *Nature* **2007**, *448*, 325–330.
(49) Wen, W. Y.; Wang, W. N.; Zhang, M. J. *Curr. Top. Med. Chem.* **2006**, *6*, 711–721.